DMD Fast Forward. Published on June 3, 2013 as doi: 10.1124/dmd.112.049585

DMD #49585

NANOPARTICLE FORMULATION OF A POORLY SOLUBLE CB-1 ANTAGONIST IMPROVES ABSORPTION BY RAT AND HUMAN INTESTINE

Sanna Siissalo, Hans de Waard, Marina H. de Jager, Rose Hayeshi, Henderik W. Frijlink, Wouter L.J. Hinrichs, Heike Dinter-Heidorn, Annie van Dam, Johannes H. Proost, Geny M.M. Groothuis, Inge A.M. de Graaf

Division of Pharmacokinetics, Toxicology, and Targeting, Department of Pharmacy, University of Groningen, Antonius Deusinglaan 1, 9713 AV Groningen, The Netherlands: S.S., M.H.J., R.H., J.H.P., G.M.M.G., I.A.M.G.

Division of Pharmaceutical Technology and Biopharmacy, Department of Pharmacy, University of Groningen, Antonius Deusinglaan 1, 9713 AV Groningen, The Netherlands: H.W.,H.W.F., W.L.J.H.

Abbott Products GmbH, Hans-Böckler-Allee 20, 30173 Hannover, Germany: H.D-H.

Mass Spectrometry Core Facility, University of Groningen, Antonius Deusinglaan 1, 9713 AV Groningen, The Netherlands: A.D.

Running Title: Nanoparticles of poorly soluble CB-1 antagonist

Corresponding author:
Prof.dr.G.M.M.Groothuis
Antonius Deusinglaan 1
9713 AV Groningen (the Netherlands)
Tel.: +31 50 363 3313
Fax: +31 50 363 3247
email: g.m.m.groothuis@rug.nl

#text pages **32**

 # tables **2**

 # figures **8**

 # references **22**

#word in abstract: **251**

#words in introduction **625**

#words in discussion **1058**

List of non-standard abbreviations

AUC: area under the curve

BCS: Biopharmaceutics Classification System

CB-1: Cannabinoid receptor 1

DMSO: dimethylsulfoxide

DSC: differential scanning calorimetry

NMP: N-methyl-2-pyrrolidone

EM: electron microscopy

TBA: tertiary butyl alcohol

XRPD: X-ray powder diffraction

Abstract

The inclusion of nanoparticles dispersed in a hydrophilic matrix is one of the formulation strategies to improve the bioavailability of orally administered BCS class II and IV drugs by increasing their dissolution rate in the intestine. To confirm that the increased dissolution rate results in increased bioavailability, *in vitro* and *in vivo* animal experiments are performed, however, translation to the human situation is hazardous. In this study, we used a range of *in vitro* and *ex vivo* methods, including methods applying human tissue, to predict the *in vivo* oral bioavailability of a model BCS class II CB-1 antagonist, formulated as a nanoparticle solid dispersion. The enhanced dissolution rate from the nanoparticle formulation resulted in an increased metabolite formation in both rat and human precision-cut intestinal slices, suggesting increased uptake and intracellular drug concentration in the enterocytes. In Ussing chamber experiments with human tissue both the metabolite formation and apical efflux of the metabolite were increased for the nanoparticulate solid dispersion compared to a physical mixture, in line with the results in intestinal slices. The pharmacokinetics of the different formulations was studied in rats *in vivo*. The nanoparticle formulation indeed improved the absorption of the CB-1 antagonist and the delivery into the brain compared to the physical mixture. In conclusion, the combined approach provides a valuable set of tools to investigate the effects of formulation on the absorption of poorly soluble compounds in human intestine and may provide relevant information on the oral bioavailability in humans early in the development process.

DMD Fast Forward. Published on June 3, 2013 as DOI: 10.1124/dmd.112.049585
This article has not been copyedited and formatted. The final version may differ from this version.

Introduction

Many new drug candidates can be categorized as class II drugs according to the Biopharmaceutics Classification System (BCS) (Lipinski et al., 2001, Amidon et al., 1995). These drugs have a good permeability but a low oral bioavailability due to their low dissolution rate. Therefore, the oral bioavailability can be improved by increasing the dissolution rate (Curatolo, 1998).

One of the strategies to deal with solubility problems is to increase the dissolution rate by using nanoparticulate solid dispersions (Jinno et al., 2006; Visser et al., 2010). The dissolution rate is enhanced by the increased surface area (Noyes-Whitney equation) (Noyes and Whitney, 1897), the decreased thickness of the diffusion boundary layer (Prandtl equation) (Bisrat and Nyström, 1988), and the increased saturation concentration around the small particles (Kelvin and Ostwald-Freundlich equation) (Hou et al., 2003).

Previously, we developed a novel bottom-up process to produce drug nanoparticles (de Waard et al., 2008). To prepare drug nanoparticles by this process, a drug and a matrix material, dissolved in a mixture of tertiary butyl alcohol (TBA) and water is rapidly frozen and subsequently freeze-dried.

The dissolution behavior of an unprocessed model compound and of the model compound formulated as nanoparticulate solid dispersion is commonly studied in *in vitro* dissolution experiments. Although such *in vitro* dissolution tests can indeed show an enhanced dissolution rate, it does not necessarily provide proof of improved intestinal permeability in human intestine especially when metabolic enzymes and transporters are involved (Martinez and Amidon, 2002). *In vivo* studies in rat may provide information on intestinal permeability, but the extrapolation to the human situation is hazardous due to interspecies differences in permeability, metabolism, and transporter activities. Caco-2 cells are frequently used to study intestinal absorption, but these cells do not contain physiological

levels of the drug metabolizing enzymes and drug transporters and, thus, it is difficult to predict bioavailability in humans from the results of these experiments (Sun et al., 2002).

In this study, we investigated whether the potentially increased bioavailability after formulation of a BCS class II drug as a nanoparticulate solid dispersion can be predicted by applying *in vitro* dissolution experiments and *ex vivo* models for absorption and metabolism with human intestinal tissue. An experimental Cannabinoid Receptor-1 (CB-1) antagonist was chosen as a model compound for a BCS class II drug (aqueous solubility of less than 10 mg/L) (Figure 1). CB-1 antagonists were originally developed for the treatment of obesity and, consequently, prevention of the related cardiometabolic disorders (Bifulco et al., 2009). The therapeutic applicability of our CB-1 antagonist is limited by its low solubility and dissolution rate and thus low bioavailability. Therefore, we studied uptake and metabolism of the CB-1 antagonist, formulated as nanoparticulate solid dispersion, in two human *ex vivo* preparations of intestine: precision-cut intestinal slices and Ussing chambers. Precision-cut intestinal slices are an established tool for drug metabolism and toxicology studies (de Graaf et al.,2010, Possidente et al., 2011, van de Kerkhof et al., 2005, van de Kerkhof et al., 2006), but they do not give direct information on vectorial transport and bioavailability. Ussing chambers have been used to study transport of drugs across the intestinal tissue (Söderholm et al., 1998). Recently, they were also used to study intestinal metabolism, allowing for the monitoring of the mucosal and serosal excretion separately (van de Kerkhof et al., 2006).

In this study, these two techniques (precision-cut slices and Ussing chambers) were employed using human and rat jejunum to investigate the improved absorption of the model CB-1 antagonist administrated as a nanoparticulate solid dispersion compared to a physical mixture. Furthermore, the *in vitro* and *ex vivo* observations in rat slices were confirmed in *in vivo* pharmacokinetic studies in the rat, where bioavailability and brain distribution were measured after administration of the different formulations of the CB-1 antagonist

DMD Fast Forward. Published on June 3, 2013 as DOI: 10.1124/dmd.112.049585
This article has not been copyedited and formatted. The final version may differ from this version.

Materials and Methods

Materials

Mannitol was obtained from Roquette (France). Williams Medium E + Glutamax^{TM} –I and gentamycin were purchased from Invitrogen (Paisley, UK), fungizone from Bristol-Myers-Squibb (New York, NY, USA) and glucose monohydrate from Merck (Darmstadt, Germany).

The model CB-1 antagonist E-3-(4-chlorophenyl)-N-methyl-4-phenyl-N'-(4-(trifluoromethyl)piperidin-1-ylsufonyl)-4,5-dihydro-1H-pyrazole-1-carboxamidine belonging to the group of 3,4-Diarylpyrazoline CB1 receptor antagonists, (Lange *et al* 2010) was donated by Abbott Products GmbH (formerly Solvay Pharmaceuticals, Hannover, Germany). All the other reagents were of the highest quality commercially available.

Animals and tissue

Human jejunum

Human jejunum tissue (2 male and 2 female) was obtained from pancreatoduodenectomies performed at the University Medical Center Groningen (the Netherlands). The resected pieces of jejunum were stored in ice-cold oxygenated Krebs-Henseleit buffer and transported to the laboratory within 15 minutes after excision of the tissue as described before (de Graaf et al., 2010).

Rat jejunum

Rat jejunum tissue was obtained from nonfasted male Wistar rats (Charles River, Germany) and prepared for slicing as described before (de Graaf et al., 2010).

Rats for in vivo experiments

Male Wistar rats (Charles River, Kissleg, Germany) of 250-450 g were housed under a 12 h dark/light cycle at constant humidity and temperature. Animals were permitted free

DMD Fast Forward. Published on June 3, 2013 as DOI: 10.1124/dmd.112.049585
This article has not been copyedited and formatted. The final version may differ from this version.

access to tap water and standard lab chow. All experiments were approved by the committee for care and use of laboratory animals of Abbott GmbH& Co.KG in Ludwigshafen and were performed according to strict governmental and international guidelines.

Methods

Preparation of the nanoparticulate solid dispersion

The nanoparticulate solid dispersions were prepared according to a previously described method (de Waard et al., 2008). Briefly, separate solutions of the drug in TBA (12.5 mg/mL) and mannitol (the matrix material) in water (see table 1 for compositions) were heated to approximately 60 ºC. Of the heated drug solution, 0.8 mL was added to 1.2 mL of the heated mannitol solution and mixed in a glass vial. Immediately after mixing, the sample was frozen in liquid nitrogen. Then, the frozen samples were placed on a pre-cooled (-50 ºC) freeze-dryer shelf. This temperature was maintained for 1.5 hours, after which the temperature was increased to -25 ºC for the duration of three hours. Finally the samples were dried for 10 hours at 0.220 mBar. After gradually increasing the temperature to room temperature, the powders were removed from the freeze-dryer and stored in a desiccator over silica gel.

The conventional formulation in the *in vitro* experiments was a physical mixture of the unprocessed drug and mannitol prepared using a spatula and mortar.

Tabletting

For the *in vivo* studies, the powders were compressed into 5x2 mm oblong tablets having a weight of 25 mg on an ESH compaction apparatus (Hydro Mooi, Appingedam, The Netherlands). The tablets contained 3 mg of drug. Three tablets were prepared during each compaction cycle. The used compaction rate was 0.5 kN/s and the maximum compaction load was 6 kN. The obtained tablets were stored in a desiccator over silica gel at room temperature for at least 1 day before further processing.

Physical characterization

The crystallinity and morphology of the unprocessed drug and the freeze-dried powder were determined by differential scanning calorimetry (DSC), X-ray powder diffraction (XRPD), and scanning electron microscopy (EM). For DSC, a Q2000 scanning calorimeter (TA Instruments, Ghent, Belgium) was used. The samples (1-10 mg) were heated at a rate of 2 ºC from -50 to 200 ºC. For XRPD, a D2 Phaser diffractometer (Bruker, Karlsruhe, Germany) was used. The sample powder were dispersed on a silicium zero-background sample holder and scanned from 5-60 º2θ with step size of 0.004 º2θ and a time per step of 0.5 s. For SEM, a JEOL JSM 6301-F microscope (JEOL, Japan) was used. The sample powders were dispersed on top of double-side sticky carbon tape on metal disks and coated with a thin layer of gold/palladium.

Dissolution experiments

The dissolution rate of the CB-1 antagonist from the tablets was determined in a USP dissolution apparatus II (Sotax AT 7, Basel, Switzerland). One L 0.5% w/v sodium lauryl sulphate solution at 37 ºC was used as dissolution medium. The paddle speed was set at 100 rpm. The concentration of dissolved drug was measured spectrophotometrically (Evolution 300 UV-VIS spectrophotometer, Thermo Fisher Scientific, Madison, U.S.A.) at a wavelength of 312 nm.

Precision-cut intestinal slices

Precision-cut intestinal slices were prepared from rat and human jejunum tissue according to the published protocol (de Graaf et al., 2010). Briefly, intestinal tissue was embedded in 3% (w/w) agarose cylinders and sliced into 4-5 mg (weight without agarose) slices with the Krumdieck tissue slicer (TSE, Bad Homburg, Germany). Slices were incubated in 12-well plates in 2.5 mL of WME intestinal slice incubation medium at 37°C in humidified carbogen atmosphere (95% O_2 / 5% CO_2) with reciprocal shaking at 90 times per minute.

At the start of the experiment, 1 mg of the nanoparticulate solid dispersions or physical mixtures containing 12 or 20 w% thus containing 0.12 or 0.20 mg of drug, respectively, were added to a well containing 2.5 mL of medium and one intestinal slice. As a reference, where dissolution was not the rate limiting step for absorption, a solution of 40 mg/ml of the physical mixture (containing 12 or 20% of the drug) in dimethylsulfoxide (DMSO) was prepared to yield solutions with drug concentrations of 4.8 and 8 mg/mL, respectively. Of these solutions, 25 µl (thus containing 0.12 and 0.20 mg of drug) was added to each well containing 2.5 mL of medium and one intestinal slice. For all formulations (nanoparticulate dispersion, physical mixture and reference solution) the total amount of the drug in the wells was the same. DMSO concentration in the medium was <1%. Samples of 100 µL were taken after 3 hours of incubation, immediately centrifuged and 50 µL of the supernatant was transferred to another tube for metabolite analysis. At the end of the incubation (3 h) the slices were collected and stored at -20°C until the determination of their content of CB-1 antagonist and its metabolites.

Ussing chambers

A sheet of human tissue, prepared as described for the preparation of precision-cut intestinal slices before (de Graaf et al., 2010) was further processed by removing all the remaining submucosal tissue. The mucosa was cut into approximately 1 cm squares, which were mounted into EasyMount #2410 inserts (Harvard Apparatus GmbH, Hugstetten, Germany). Inserts were then placed in EasyMount #2400 chambers (Harvard Apparatus GmbH, Hugstetten, Germany) and 2.5 mL of Krebs-Ringer-buffer (115 mM NaCl, 25 mM $NaHCO_3$, 2.4 mM K_2HPO_4, 0.4 mM KH_2PO_4, 1.2 mM $MgCl_2$, 1.2 mM $CaCl_2$ and 10 mM glucose) was added to both sides and the tissue and heated to 37 ºC. Humidified carbogen (95% O_2 / 5% CO_2) was bubbled through the chambers. The electrical parameters, potential difference and resistance across the tissue, were monitored with Clamp software (Scientific

Instruments, Aachen, Germany) through standard EasyMount electrodes in tips completely filled with 4% (w/w) agar-agar in Krebs-Ringer-buffer without glucose and were stable during the incubation period, indicating viability of the tissue.

After 30 minutes of stabilization, the experiment was initiated by adding the formulations containing 1 mg of the drug or 25 µL of the 100x concentrated stock solution in DMSO in the apical chamber. Samples of 100 µL were taken from the apical and basolateral compartment at 3 hours, immediately centrifuged and 50 µL of the supernatant was transferred to another tube. At the end of the incubation (3 h) the tissue was collected and stored at -20°C until the determination of the tissue content of the CB-1 antagonist and/or its metabolites.

In vivo pharmacokinetics in rats

Male Wistar rats were used for *in vivo* comparison of the pharmacokinetics of three formulations: 1) the reference formulation (2.5 mg ml^{-1}) consisting of CB-1 antagonist dissolved in N-methyl-2-pyrrolidone (NMP; Pharmasolve, ISP, Germany), which was heated and mixed with ultrapure water (65:35 v/v); 2) a 25 mg tablet composed of the physical mixture containing 3 mg of the crystalline CB-1 antagonist and mannitol; 3) a 25 mg tablet composed of the nanoparticulate solid dispersion containing 3 mg of the CB-1 antagonist. The dose administered to the rats was 10 mg/kg for all formulations. The reference solution was orally administered to the rat (4 ml/kg). The tablets containing the nanoparticulate solid dispersion or the physical mixture were put into size 9 rat capsules immediately before application to avoid water absorption (by the tablet from the gelatin) and administered to rats using a dosing syringe from a PCcapsTM KIT (Capsugel, Belgium). Afterwards, 3mL/kg tap water was administered to each rat by oral gavage. After each time point of 30 min, 1, 3, 7 and 24 h the animals (n=3 for each time point) were anaesthetized using isoflurane and sacrificed, and plasma (by cardiac puncture) and brain were collected. Phosphate buffered

saline was added to the brain (8 v/w) and the tissue was homogenized using the Geno/Grinder (Spex Sample Prep, USA). Protein in the samples was precipitated by addition of 400 µL acetonitrile to 100 µL of brain homogenate or 50 µL plasma, and the samples were spun down at 2000g for 10 minutes. Supernatant was diluted 1:1 with 10 mM ammonium acetate (pH 3) and the concentration of the CB-1 antagonist as well as the peak area for the metabolite in brain and plasma were determined using LC-MS/MS, and subsequently, the brain/plasma concentration ratios were calculated for the different treatment groups.

LC-MS/MS analyses

For the *ex vivo* experiments the CB-1 antagonist and its metabolites HPLC was performed using a Shimadzu LC system, consisting of a SIL-20AC autosampler and two LC-20AD gradient pumps. Chromatographic separation was achieved at room temperature on a Kinetex C18 column (2.1x50 mm, 2.6 µm particles from Phenomenex. Eluent A was 100% H2O and eluent B was 100% methanol, both containing 0.1% (v/v) formic acid. The elution was performed starting at 40% B, followed by a linear gradient to 85% B and then in 3 min followed by a linear gradient to 86% B in 1 min. Then, the column was washed with 98% B for 4 min after which it was returned to the starting conditions. The flow rate was 0.4 mL/min. The injection volume was 50 µL. The HPLC system was coupled to an API 3000 triple-quadrupole mass spectrometer (Applied Biosystems/MDS Sciex) equipped with a TurboIonSpray source. The ionization was performed by electrospray in the positive mode. The TurboIonSpray temperature was 450˚C. Nitrogen was used as turbo heater gas, nebulizer gas and curtain gas. Full scan spectra were acquired to detect metabolites of S310. They were recorded at a scan time of 2 s with a scan range of m/z 100-1100 and a step size of 1. For the semi-quantitative measurements MS/MS fragmentation was carried out for each metabolite to determine the selected reaction monitoring (SRM) ion pairs (528.2/375.1 for S310 and

560/255 for the metabolite). Warfarin was used as internal standard. Data were collected and analyzed with Analyst 1.5.1 software (Applied Biosystems/MDS Sciex).

The residual CB-1 antagonist and the metabolite retained in the tissue at the end of the *ex vivo* experiments were determined by homogenizing the tissues by sonication (2 x 15s) in 100 µL of intestinal slice incubation medium followed by centrifugation (2 min, 16,1 g) and measuring the supernatants as described above.

For the *in vivo* experiments, the concentrations of the CB-1 antagonist, and peak areas of the metabolite were measured using an Ab Sciex 5500 Qtrap and compounds were separated on a Phenomenex Kinetex C18 column (2.1 x 30 mm, 2.6 µm particle size). The elution gradient was: 0 min 1% B, 0.4 min 99% B, 1.5 min 99% B, 1.51 min 1% B. Solvent A consisted of 10 mM ammonium acetate (pH 3) and solvent B of 100% acetonitrile. Flow rate was 900 µL/min and the capillary temperature was set at 950°C. Positive electrospray ionization was achieved using a nitrogen sheath gas with ionization voltage at 5.5 kV. Detection of each analyte was based on isolation of the protonated molecular ion, $[M+H]^+$ and subsequent MS/MS fragmentations and a selected reaction monitoring were carried out. An internal standard was used to determine the concentration of the CB-1 antagonist (Q1/Q3 masses 527.85/374.00). The lower limit of quantification was 1.06 ng/mL for the CB-1 antagonist.

Calculation of pharmacokinetics and Statistical analysis

All ex vivo experiments were performed with a minimum of 3 intestines, using 2 pieces for Ussing chambers experiments and/or 3 slices from each intestine, unless indicated otherwise. Results were compared using a two-tailed paired or unpaired Student's t-test where appropriate. The criterion for significance was a p value <0.05.

For determination of the area under the curve (AUC) in plasma and brain data of 18 rats (3 rats on each time-point) were taken into account. The AUC of n data pairs (C_i,t_i)

(i=1,2,..,n) can calculated using the trapezoidal rule, approximating the concentration between measurements by a straight line:

$$AUC = \sum_{i=1}^{n-1} \frac{1}{2} \cdot (C_i + C_{i+1}) \cdot (t_{i+1} - t_i) \quad (1)$$

Eq. (1) can be rearranged to:

$$AUC = \sum_{i=1}^{n} \frac{1}{2} \cdot C_i \cdot \Delta t_i \quad (2)$$

where Δt_i equals $(t_2 - t_1)$ for i=1, $(t_n - t_{n-1})$ for i=n, and $(t_{i+1} - t_{i-1})$ for 1<i<n.

Eq. 2 shows that AUC is a linear function of the concentrations C_i (i=1,2,..,n). Therefore the variance of AUC can be calculated from the variances in C_i according to the law of propagation of errors (Mandel, 1964):

$$var(AUC) = \sum_{i=1}^{n} var(C_i) \cdot \left(\frac{dAUC}{dC_i} \right)^2 \quad (3)$$

From Eq. (2) the derivatives of AUC with respect to C_i can be derived by differentiation:

$$\frac{dAUC}{dC_i} = \frac{1}{2} \cdot \Delta t_i \quad (4)$$

Substituting Eq. (4) in Eq. (3) results in:

DMD Fast Forward. Published on June 3, 2013 as DOI: 10.1124/dmd.112.049585
This article has not been copyedited and formatted. The final version may differ from this version.

$$\mathrm{var}(AUC) = \sum_{i=1}^{n} \mathrm{var}(C_i) \cdot \left(\frac{1}{2} \cdot \Delta t_i \right)^2 \qquad (5)$$

Statistical significance was determined by testing the hypothesis deltaAUC= AUC(dosage form 1)-AUC (dosage form 2) ≠ 0, with 95% confidence.

$T_{1/2}$ could not be calculated due to the limited amount of data-points on the descending part of the concentration/time profile for the nanoparticle formulation.

Results

DSC and XRPD showed that the unprocessed drug was crystalline while the drug in the nanoparticulate dispersion was amorphous (data not shown). In Figure 2 scanning EM pictures of the unprocessed drug and the nanoparticulate solid dispersion are shown. As can be seen, the unprocessed drug consists of long needle-shaped crystals with a length varying from a few μm to hundreds of μm. The nanoparticulate solid dispersion consists of the drug and the carrier mannitol. Because in the EM pictures we cannot distinguish between the two components, the particle size of the drug cannot be given. However, it is clear from the pictures that all particles, drug and mannitol, are smaller than 1 μm. Hence, the drug particles are in the nanometer range and therefore much smaller than the unprocessed drug. Compared to the physical mixture, the *in vitro* dissolution of the CB-1 antagonist was both faster and more extensive from the nanoparticulate solid dispersion containing tablet (Figure 3). The amount of CB-1 antagonist dissolved from the tablets composed of the physical mixture after 2 hours was just 25%, while 100% was dissolved within 5 minutes from the nanoparticulate solid dispersion.

As vectorial transport cannot be measured in slices, the influence of the formulation type on the metabolite formation was taken as a surrogate for the amount of drug taken up in the tissue in human and rat jejunum, assuming that the free drug concentrations were below enzyme saturation. After the incubation of the CB-1 antagonist (m/z 528, retention time 3.42 min4) with either rat or human intestinal slices, only one metabolite of the CB-1 antagonist was found using LC-MS/MS analysis. This metabolite caused two peaks with molecular weights of +32 (m/z 560, retention time 2.59 min,) and +14 (m/z 542, retention time 2.59 min) corresponding to a di-hydroxylated metabolite and loss of water from the molecule in the MS. The absolute quantification of the metabolite was not possible as this metabolite was not available as pure compound.

In both species, significantly higher metabolite levels were observed following the administration of the nanoparticulate solid dispersion compared to the physical mixture. The metabolite levels after administration of the nanoparticulate solid dispersion reached 38% in human tissue and 72 % in rat tissue of the amount metabolized after administration of the compound dissolved in DMSO (Figure 4), whereas with the physical mixture, metabolite levels reached only 3% (rat) and 11% (humans) of those obtained with the reference solution. Human metabolism of the CB-1 antagonist had a tendency to be more enhanced by the higher free drug concentration in the medium after nanoparticulate formulation (12 times) or the reference solution (31 times) as compared to the physical mixture than rat metabolism (4 and 5 times respectively), but this difference was not statistically significant ($p=0.29$ and $p=0.16$).

In Ussing chambers, an equal quantity of the CB-1 antagonist was added either as physical mixture powder, as nanoparticulate solid dispersion powder, or as solution in DMSO into the mucosal side of the Ussing chamber containing the human intestinal tissue. Formation of the di-hydroxylated metabolite of the CB-1 antagonist was significantly higher following the addition of the nanoparticulate solid dispersion into the mucosal chamber, compared to the physical mixture, reaching ca. 60 % and 5 % respectively of the amount formed after addition as dissolved in DMSO (Figure 5). There was a clear apical efflux of the metabolite into the luminal side of the Ussing chamber, whereas the excretion of the metabolite to the basolateral side was very low and was below the detection level after addition of the physical mixture. Upon analyses of the CB-1 antagonist and its metabolites retained in the tissue at the end of the experiment, a similar pattern was observed for the parent CB-1 antagonist and the metabolite: a larger amount of the compounds was retained in the tissue following the administration of nanoparticulate solid dispersion compared to the physical mixture (Figure 6). Direct measurement of the real concentration of the parent compound in the basolateral compartment was not possible due to the precipitation caused by the limited solubility of the

compound. Interestingly, the differences between the different formulations were similar in intestinal slices and Ussing chambers (compare figures 4 and 5).

To investigate whether the nanoparticulate solid dispersion improved both the absorption of the CB-1 antagonist from the intestine and the delivery into the brain, in a first *in vivo* experiment using rats, the pharmacokinetics of the CB-1 antagonist from tablets prepared from nanoparticulate solid dispersion and from physical mixture were compared with a solution of the drug in NMP which can be considered as a positive control (Tabel 2, figure 7). After administration of the physical mixture, no detectable levels of drug could be measured in plasma, whereas in the brain they were very low. However, the drug could be detected after administration of the nanoparticulate solid dispersion tablets in plasma, whereas brain levels were even approximately 20-fold higher than after administration of the physical mixture. AUCs measured after dosing with tablets containing the nanoparticulate solid dispersion reached approximately 30-40% of the levels measured after administration of the positive control in both plasma and brain, which is comparable to the difference in absorption as was measured in the in vitro experiments. A second *in vivo* experiment was performed to compare the pharmacokinetic profiles for both the metabolite and the parent compound for the tablets prepared from the nanoparticulate solid dispersion and the solution of the drug in NMP (Tabel 2, figure 7). Figure 8 shows the chromatograms the CB-1 antagonist (fig 8 A and B) and the dihydroxy-metabolite (fig 8 C and D) in plasma and brain samples respectively. The same metabolite (m/z 560/255) as was found in the ex vivo experiment was also found in plasma and brain. In this second experiment, the bioavailability (AUC) from the nanoparticulate solid dispersion calculated over 24 hours after administration was even markedly higher than from the reference solution (217 versus 29 (ng*h/mL). Analysis of the data revealed however that this high AUC was due to a very high concentration of the CB1 antagonist measured in one of the rats at t=3 hours. Since this high plasma level was not coherent

with the brain concentration of the model compound or the metabolite concentration in the plasma and brain of the same rat, the validity of this data-point is uncertain. If this data-point is not taken into account, plasma AUC after dosing with the nanoparticle solid dispersion is in a similar range (76 ng*h/mL) as resulting from dosing with the reference solution.

Similar amounts of the dihydroxy metabolite in plasma and brain were detected after dosing with both formulations (AUC of 7.7 $*10^4$ *h/mL and $1.2*10^4$ counts*h/g in the MS peak area from the liquid formulation and of 1.5 $*10^5$ *h/mL and 1.8 $*10^4$ counts*h/g from the nanoparticulate solid dispersion, respectively). Brain concentrations of the CB-1 antagonist were higher than plasma concentrations, whereas much less metabolite was found in brain than in plasma .

DMD Fast Forward. Published on June 3, 2013 as DOI: 10.1124/dmd.112.049585
This article has not been copyedited and formatted. The final version may differ from this version.

Discussion

According to the BCS, the dissolution rate is the limiting factor for the oral bioavailability of class II compounds and one of the limiting factors of class IV compounds (Amidon et al., 1995). This is a growing problem in today's drug development, since an increasing number of new drug candidates are low solubility compounds (Lipinski et al., 2001, Curatolo, 1998).

The first indications that formulating BCS class II drugs as nanoparticulate solid dispersions results in improved absorption of the model CB-1 antagonist in the present study were provided by the dissolution rate experiments, where not only the initial dissolution rate, but also the amount of dissolved drug from the nanoparticulate solid dispersion within the relevant absorption time frame of a few hours was remarkably higher than that of the physical mixture.

Indeed, the improved dissolution led to higher intracellular formation of the di-hydroxylated metabolite of the CB-1 antagonist in human intestinal tissue slices and in the Ussing chambers. Unfortunately, the absorption of the parent compound could not be measured directly due to the precipitation of the compound in the buffer at the basolateral side caused by its low solubility. However, the parent-to-metabolite ratios observed in the tissues used in the Ussing chamber experiments exhibited similar patterns: the concentrations of both CB-1 antagonist and its metabolite when administered as nanoparticles reached ~40% compared to administration as the control solution and ~5% when administered as a physical mixture, so the higher amount of the metabolite formed can indicate a higher intracellular CB-1 antagonist concentration which is an indirect indication of increased absorption.

When the drug was given as a physical mixture, human metabolism was lower than rat metabolism (data not shown), but human metabolism was more enhanced by giving the nanoparticulate dosage form (12 x, versus rat 4x) and even more by the solution in DMSO (31

x versus rat 5 x) than rat metabolism. Although these differences were not statistically significant (p=0.29 and p=0.16, respectively), there is a clear tendency for human metabolism of the CB-1 antagonist being more enhanced by a higher free concentration of the drug than rat metabolism. This observation can be explained by possible involvement of different iso-enzymes or transporters with different affinity for the model compound and a different saturation level in the different species. This empasizes the need for using human tissue to predict the effect of different dosage forms on bioavailability of drugs for human pharmacotherapy.

Strong apical efflux of the dihydroxy metabolite of the CB-1 antagonist as shown in the Ussing experiments suggests the involvement of an apical efflux transporter. Wittgen et al (2012) showed that some CB1 antagonist which are also substituted 3-(4-chlorophenyl)-4-phenyl-4,5-dihydro-1H-pyrazole-1-carboxamidine derivatives are PgP substrates and possibly MRP1 and 4 substrates but the affinity depends very much on the substituents. As the pure metabolites of the compound used in our study are not available it can only be speculated that they may be a substrate for these efflux transporters. Metabolite concentrations in the brain were considerably lower than the plasma levels. Since these metabolites are probably produced by the liver at first pass, and because these metabolites are more polar than the parent compound and possibly are substrates for apical efflux transporters present on the blood brain-barrier, they do not distribute and accumulate in the brain to the same extent as the parent compound.

All the *in vitro* and *ex vivo* observations were confirmed in the *in vivo* experiments in rats. The bioavailability of the CB-1 antagonist as shown by the concentration-time profiles was improved by the nanoparticulate solid dispersion compared to the physical mixture, from which no measurable plasma concentrations were detected. This confirms that the bioavailability of BCS class II drugs with low solubility can be improved by administration as

a nanoparticulate solid dispersion. Brain concentrations were also highly elevated by the use of the nanoparpiculate formulation. For all formulations, brain to plasma ratios of the CB-1 antagonist were strikingly high. Relatively high tissue (brain) concentrations in comparison to plasma concentrations can be explained by the high lipophilicity of our model compound and presumably because of specific binding to brain proteins or dissolution in fat in the brain. In fact high brain to plasma concentration ratios were also found for a structural analogue of our model compound (rimonabant) in other studies (Barna, 2009). High brain concentrations are probably also caused by the fact that the blood-brain barrier is not very effective for these compounds, as Wittgen et al reported that, although CB-1 structural analogues were shown to interact with efflux transporters on the blood brain barrier (MRPs, BRCP, PgP), most of them are probably not a substrate for these transporters (Wittgen, 2011; Wittgen, 2012). Moreover, there is even evidence that active uptake into the brain occurs (Barna, 2009).

We observed that peak concentrations of the CB-1 antagonist and its metabolite in brain and plasma were reached appreciably later in rats that received the nanoparticulate formulation than in rats that received the reference solution. The reason for this could be that the nanoparticulate formulation behaves as a “slow release formulation’ due to the dissolution time needed for the drug to dissolve from the nanoparticulate formulation.

In conclusion, in this study, formulation of a BCS class II compound as nanoparticulate solid dispersion was successfully used to improve the dissolution rate. This improved dissolution rate as observed *in vitro* resulted in a remarkably higher absorption and brain penetration of the model CB-1 antagonist in rat *in vivo*. This increased absorption was also observed in both *ex vivo* systems. The higher metabolite formation was indicative of the higher intracellular concentration and, thus, the improved absorption of the CB-1 antagonist. We conclude from these data that the effect of formulation on the absorption of drugs can be studied with

precision-cut intestinal slices and Ussing chambers, both allowing the use of human tissue with physiological levels of drug metabolizing enzymes and drug transporters. Species differences can be compared in precision-cut intestinal slices to validate the *in vitro-in vivo* extrapolation in a preclinical species. Our results show that formulation strategies such as the application of nanoparticulate solid dispersions may already be used in early *in vitro* and *ex vivo* screening studies providing relevant information for the *in vivo* situation. This combined approach provides a valuable tool for the prediction of formulation effects on the intestinal absorption of poorly soluble compounds in human intestine.

Acknowledgments

Dr. Vincent Nieuwenhuijs (Department of Surgery, University Medical Center Groningen) is gratefully acknowledged for the arrangements for obtaining human jejunum tissue.

Authorship Contributions.

Participated in research design: Siissalo, de Waard, Hinrichs, Frijlink, Groothuis, de Graaf.

Conducted experiments: Siissalo, de Waard, de Jager, van Dam.

Contributed new reagents or analytic tools: Hayeshi, van Dam, Dinter-Heidorn

Performed data analysis: Siissalo, de Waard, de Graaf, van Dam, Proost

Wrote or contributed to the writing of the manuscript: Siissalo, de Waard, Hinrichs, Frijlink, van Dam, Groothuis, de Graaf

References

Amidon GL, Lennernäs H, Shah VP, Crison JR (1995) Theoretical basis for a biopharmaceutical drug classification: The correlation of *in vitro* drug product dissolution and in vivo bioavailability. *Pharm Res* **12:** 413-420.

Barna I, Till I, Haller J. (2009) Blood, adipose tissue and brain levels of the cannabinoid ligands WIN-55,212 and SR-141716A after their intraperitoneal injection in mice: compound-specific and area-specific distribution within the brain. *Eur Neuropsychopharmacol.* **19(8):** 533-541.

Bifulco M, Santoro A, Laezza C, and Malfitano AM (2009) Cannabinoid receptor CB1 antagonists: state of the art and challenges. *Vitam Horm* **81:** 159-189.

Bisrat M, and Nyström C (1988) Physicochemical aspects of drug release. VIII. The relation between particle size and surface specific dissolution rate in agitated suspensions. *Int J Pharm* **47:** 223-231.

Curatolo W (1998) Physical chemical properties of oral drug candidates in the discovery and exploratory development settings. *Pharm Sci Tech Today* **1:** 387-393.

de Graaf IAM, Olinga P, de Jager MH, Merema MT, de Kanter R, van de Kerkhof EG, and Groothuis GMM (2010) Preparation and incubation of precision-cut liver and intestinal slices for application in drug metabolism and toxicity studies. *Nat Protoc* **5:** 1540-1551.

de Waard H, Hinrichs WLJ, and Frijlink HW (2008) A novel bottom-up process to produce drug nanocrystals: controlled crystallization during freeze drying. *J Control Release* **128:** 179-183.

Hou DZ, Xie CS, Huang KJ, and Zhu CH (2003) The production and characteristics of solid lipid nanoparticles. *Biomaterials* **24:** 1781-1785.

Jinno J, Kamada N, Miyake M, Yamada K, Mukai T, Odomi M, Toguchi H, Liversidge GG, Higaki K, and Kimura T (2006) Effect of particle size reduction on dissolution and oral absorption of a poorly water-soluble drug, cilostazol, in beagle dogs. *J Control Release* **111:** 56-64.

Lange JH, van der Neut MA, den Hartog AP, Wals HC, Hoogendoorn J, van Stuivenberg HH, van Vliet BJ, Kruse CG. (2010) Synthesis, SAR and intramolecular hydrogen bonding pattern of 1,3,5-trisubstituted 4,5-dihydropyrazoles as potent cannabinoid CB(1) receptor antagonists. *Bioorg Med Chem Lett*. **20(5):**1752-1757.

Lipinski CA, Lombardo F, Dominy BW, and Feeney PJ (2001) Experimental and computational approaches to estimate solubility and permeability in drug discovery and development settings. *Adv Drug Deliv Rev* **46:** 3-26.

Martinez MN, and Amidon GL (2002) A mechanistic approach to understanding the factors affecting drug absorption: A review of fundamentals. *J Clin Pharmacol **42*:** 620-643.

Mandel J, (1964) The statistical analysis of experimental data. Chapter 4. Interscience Publishers, New York.

Noyes AA, and Whitney WR (1897) The rate of solution of solid substances in their own solutions. *J Am Chem Soc* **19:** 930-934.

Possidente M, Dragoni S, Franco G, Gori M, Bertelli E, Teodori E, Frosini M, and Valoti M (2011) Rat intestinal precision-cut slices as an *in vitro* model to study xenobiotic interaction with transporters. *Eur J Pharm Biopharm* **79:** 343-348.

Söderholm JD, Hedman L, Artursson P, Franzén L, Larssen J, Pantzar N, Permert J, Olaison G (1998) Integrity and metabolism of human ileal mucosa *in vitro* in the Ussing chamb er. *Acta Physiol Scand* **162:** 47-56.

Sun D, Lennernäs H, Welage LS, Barnett JL, Landowski CP, Foster D, Fleisher D, Lee K-D, and Amidon GL (2002) Comparison of human duodenum and Caco-2 gene expression profiles for 12,000 gene sequences tags and correlation with permeability of 26 drugs. *Pharm Res* **19:** 1400-1416.

van de Kerkhof EG, de Graaf IAM, de Jager MH, Meijer DKF, and Groothuis GMM (2005) Characterization of rat small intestinal and colon precision-cut slices as an in vitro system for drug metabolism and induction studies. *Drug Metab Dispos* ***33*:** 1613-1620

van de Kerkhof EG, Ungell AL, Sjöberg AK, de Jager MH, Hilgendorf C, de Graaf IAM, and Groothuis GMM (2006) Innovative methods to study human intestinal drug metabolism in

vitro: precision-cut slices compared with ussing chamber preparations. *Drug Metab Dispos* **34:** 1893-1902.

Visser MR, Baert L, van't Klooster G, Schueller L, Geldof M, Vanwelkenhuysen I, de Kock H, De Meyer S, Frijlink HW, Rosier J, and Hinrichs WLJ (2010) Inulin solid dispersion technology to improve the absorption of the BCS Class IV drug TMC240. *Eur J Pharm Biopharm* **74:** 233-238.

Wittgen HG, van den Heuvel JJ, van den Broek PH, Dinter-Heidorn H, Koenderink JB, Russel FG (2011) Cannabinoid type 1 receptor antagonists modulate transport activity of multidrug resistance-associated proteins MRP1, MRP2, MRP3, and MRP4. *Drug Metab Dispos*. **39(7):**1294-302

Wittgen HG, Greupink R, van den Heuvel JJ, van den Broek PH, Dinter-Heidorn H, Koenderink JB, Russel FG (2012) Exploiting transport activity of p-glycoprotein at the blood-brain barrier for the development of peripheral cannabinoid type 1 receptor antagonists. *Mol Pharm*. **9(5):**1351-1360.

Footnotes.

This study was performed within the framework of project T5-105 of and financed by the Dutch Top Institute Pharma.

Address for reprint requests:

Prof.dr.G.M.M.Groothuis
Antonius Deusinglaan 1
9713 AV Groningen (the Netherlands)
Tel.: +31 50 363 3313
Fax: +31 50 363 3247
email: g.m.m.groothuis@rug.nl

[1]Present address of dr. Rose Hayeshi: Council for Scientific and Industrial Research, Polymers and Composities, P.O. Box 395, Pretoria 0001, South Africa

LEGENDS TO FIGURES

Figure 1. Molecular structure of the model CB-1 antagonist.

Figure 2. Scanning EM pictures of the pure drug (left) and nanoparticulate solid dispersion (right). The nanoparticulate dispersion contains 12% w/w of the model drug.

Figure 3. Dissolution profiles of the CB-1 antagonist from tablets composed of the physical mixture (squares) and the nanoparticles (circles). The tablets contained 12% w/w (closed symbols) or 20% w/w (open symbols) CB-1 antagonist (n = 3; mean ± standard deviation).

Figure 4. CB-1 antagonist metabolite formed in human (n=3) and rat (n=3) intestinal slices during 3h incubation with the different formulations, expressed as % of the metabolite formed in the incubation with the reference solution. Data-points reflect mean + standard deviation. *Statistically significant from the reference solution, †Statistically significant from the nanoparticulate solid dispersion ($p<0.05$).

Figure 5. CB-1 antagonist metabolite formed in human tissue (n = 4) in Ussing chambers and excreted into the apical and basolateral sides of the tissue during 3h incubation with the different formulations, expressed as % of the metabolite excreted into the apical side in the incubation with the reference solution. Data-points reflect mean + standard deviation. *Statistically significant from the reference solution, †statistically significant from the nanoparticulate solid dispersion, $^{\$}$statistically significant from the apical chamber ($p<0.05$).

Figure 6. CB-1 antagonist and the metabolite retained in the tissue after 3h incubation of human tissue in Ussing chambers (n=2) with the different formulations, expressed as % of the residual CB-1 antagonist or metabolite at 3h incubation with the reference solution. Data-points reflect mean + standard deviation. *Statistically significant from the reference solution, †statistically significant from the nanoparticulate solid dispersion ($p<0.05$).

Figure 7. Concentration-time profiles of the CB1 antagonist and its di-hydroxymetabolite in brain and plasma after in vivo treatment of rats with the different dosage forms. Data-points reflect average values of 3 rats that were sacrificed at the indicated time-points. (A) Plasma levels of the CB1 antagonist, study 1 (B) Brain levels of the CB1 antagonist, study 1 (C) Plasma levels of the CB1 antagonist, study 2 (D) Brain levels of the CB1 antagonist, study 2 (E) Plasma levels of the di-hydroxymetabolite, study 2 (F) Brain levels of the di-hydroxymetabolite, study 2.

Figure 8. MS chromatogram of the CB-1 antagonist (m/z 528>375) and its di-hydroxy-metabolite (m/z 560>522) in plasma and brain after dosing of the reference solution. A) CB-1 antagonist in plasma B) CB-1 antagonist in brain C) di-hydoxymetabolite in plasma D) di-hydroxymetabolite in brain.

DMD Fast Forward. Published on June 3, 2013 as DOI: 10.1124/dmd.112.049585
This article has not been copyedited and formatted. The final version may differ from this version.

TABLES

Table 1. Composition of the different solutions used for freeze-drying. In all experiments 1.2 mL aquous solution was mixed with 0.8 mL TBA solution (i.e. ratio of 6/4).

Before freeze-drying		After freeze-drying
$C_{drug/TBA}$ (mg/mL)	$C_{mannitol/water}$ (mg/mL)	Drug load (% w/w)
12.5	61.1	12
12.5	33.3	20

Table 2. AUC's of the CB1-antagonist and its major metabolite in plasma and brain of rats that received various dosage forms.

		Study I		
		Physical mixture	Nanoparticulate solid dispersion	Reference solution
Parent	Plasma (ng*h/ml)	0 ±0*	14 ± 11	45 ± 18
	Brain (ng*h/g)	34 ± 19†	863 ± 143	2257 ± 559††
		Study II		
		Physical mixture	Nanoparticulate solid dispersion	Reference solution
Parent	Plasma (ng*h/ml)	ND	217 ± 246	18 ± 11
	Brain (ng*h/g)	ND	1949 ± 404	1008 ± 453
Metabolite	Plasma (counts*h/ml)	ND	$1.5x10^5 \pm 9.2x10^4$	$7.7x10^4 \pm 3.2x10^4$
	Brain (counts*h/g)	ND	$1.8x10^4 \pm 9.9x10^3$	$1.2x10^4 \pm 3.9x10^3$

*Values represent average AUC±SD
ND: not determined
†Significantly lower than nanoparticulate solid dispersion
††Significantly higher than nanoparticulate solid dispersion

DMD Fast Forward. Published on June 3, 2013 as DOI: 10.1124/dmd.112.049585
This article has not been copyedited and formatted. The final version may differ from this version.

Figure 1

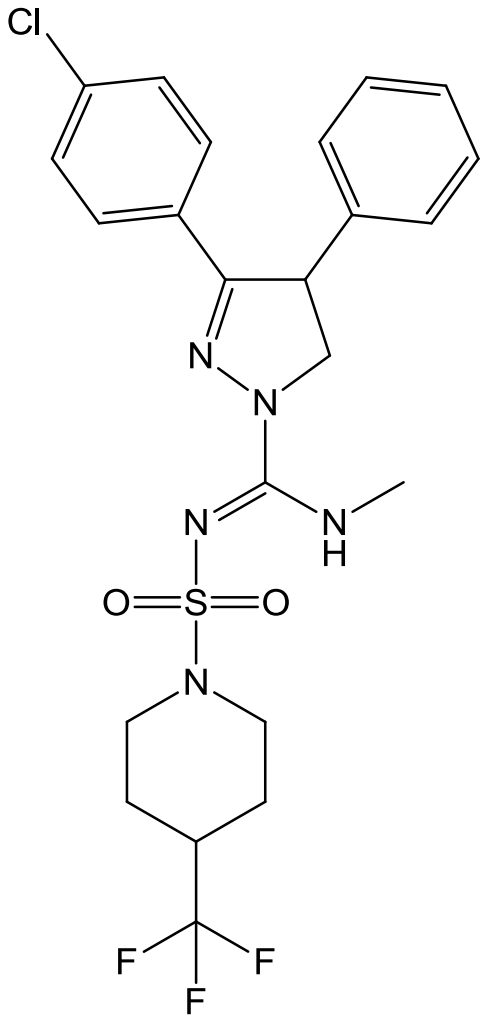

DMD Fast Forward. Published on June 3, 2013 as DOI: 10.1124/dmd.112.049585
This article has not been copyedited and formatted. The final version may differ from this version.

Figure 2

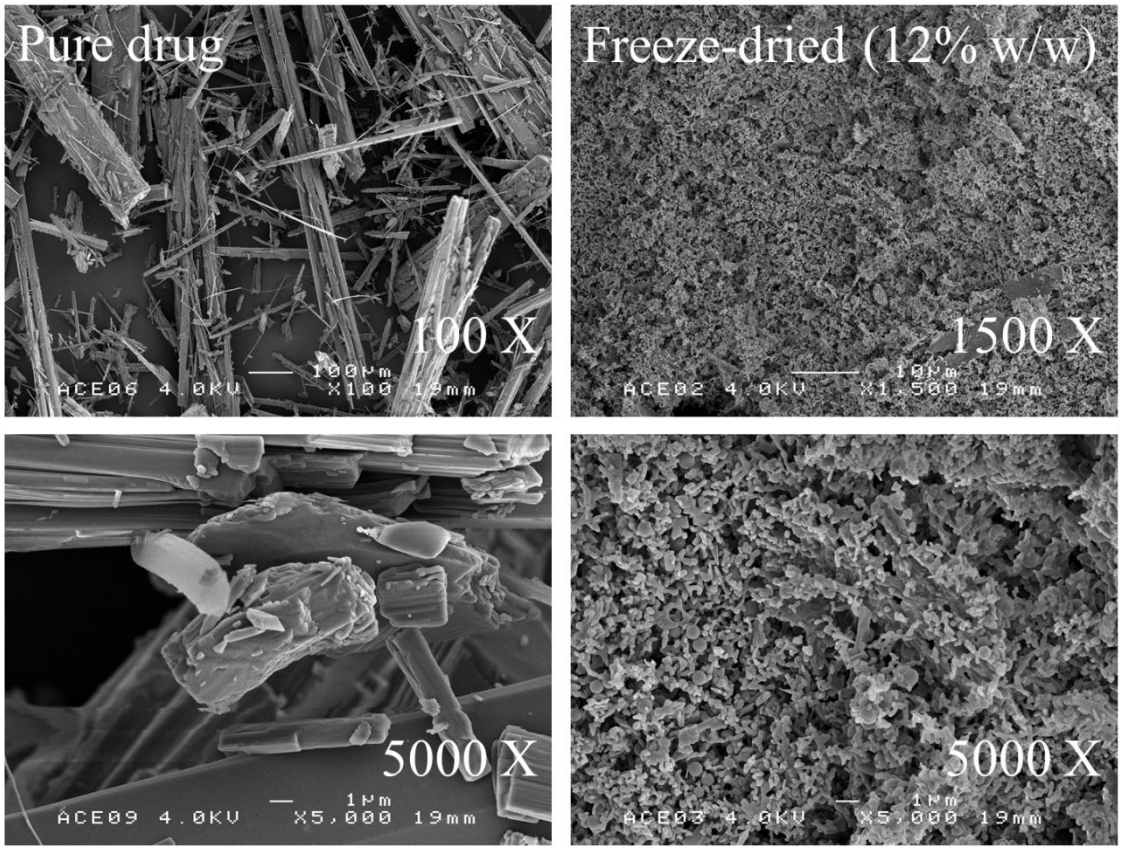

DMD Fast Forward. Published on June 3, 2013 as DOI: 10.1124/dmd.112.049585
This article has not been copyedited and formatted. The final version may differ from this version.

Figure 3

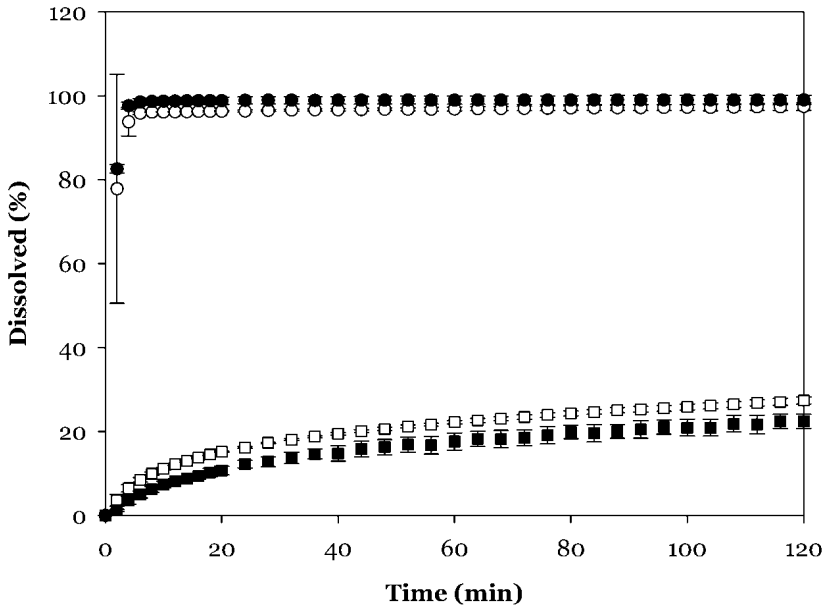

Figure 4

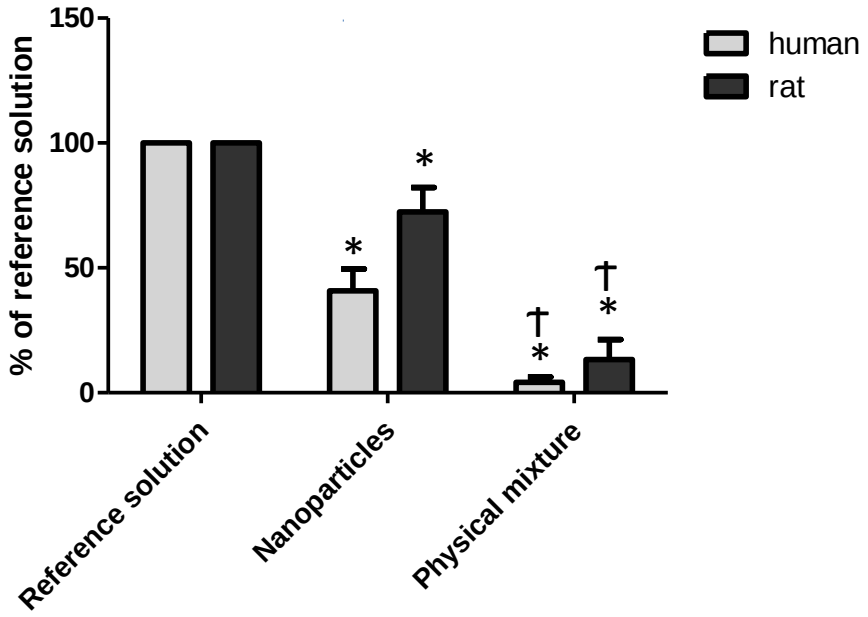

Figure 5

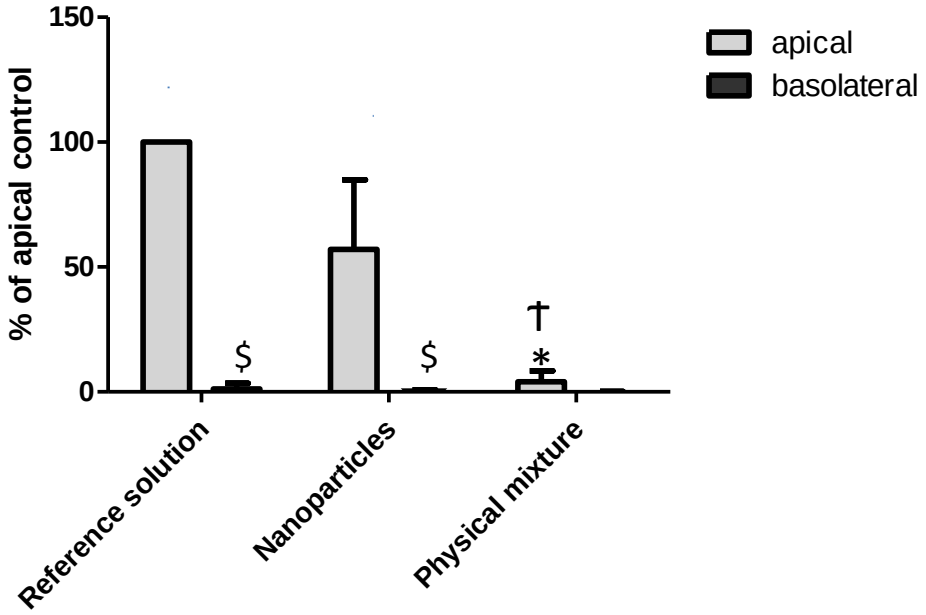

Figure 6

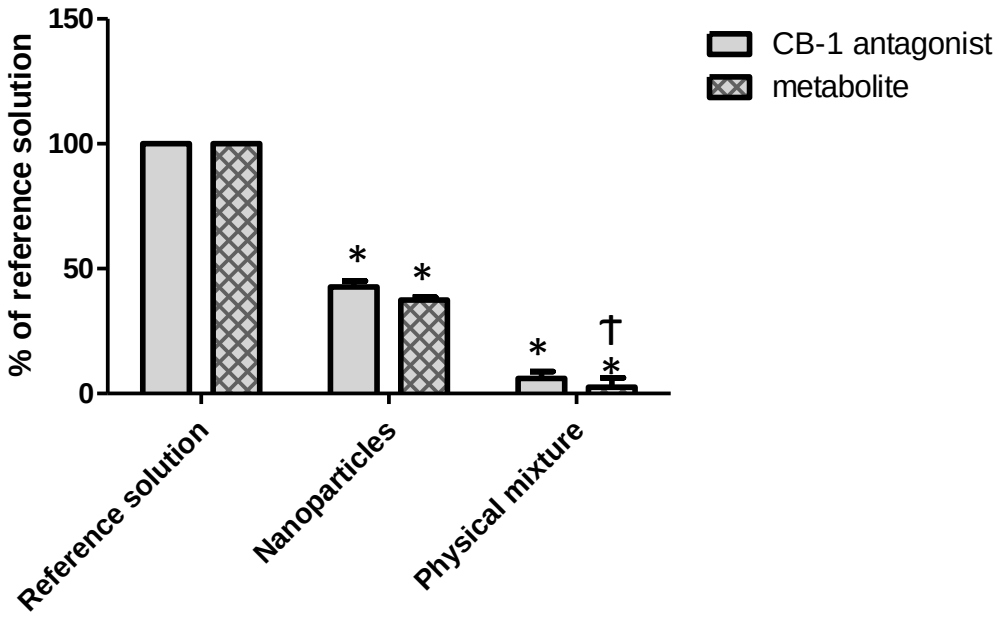

Figure 7

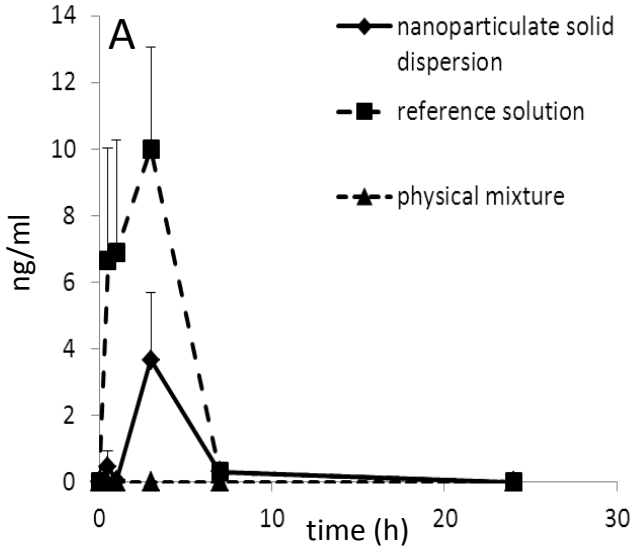
A
nanoparticulate solid dispersion
reference solution
physical mixture
ng/ml
time (h)

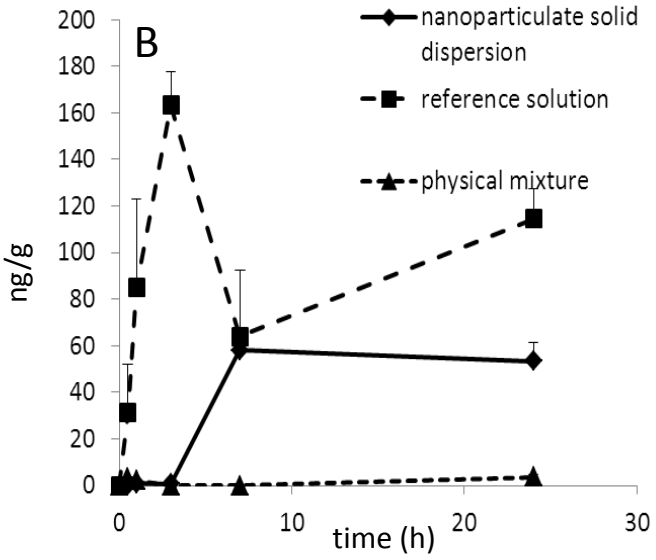
B
nanoparticulate solid dispersion
reference solution
physical mixture
ng/g
time (h)

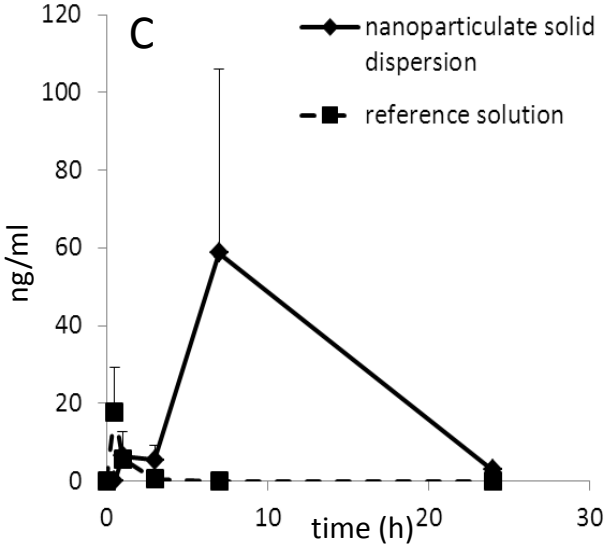
C
nanoparticulate solid dispersion
reference solution
ng/ml
time (h)

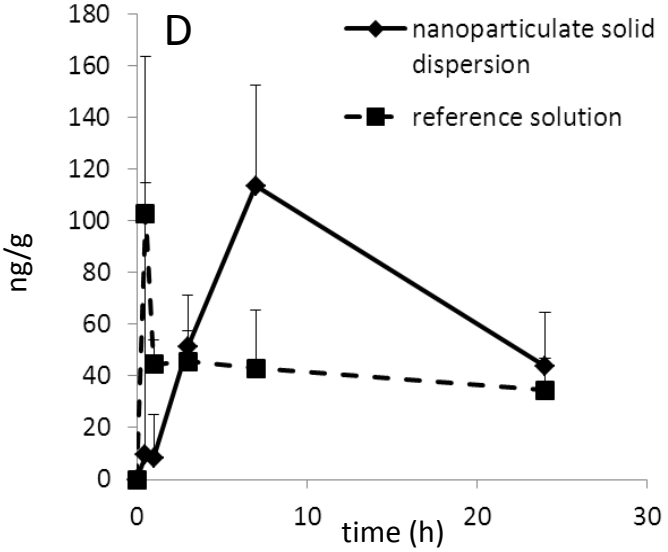
D
nanoparticulate solid dispersion
reference solution
ng/g
time (h)

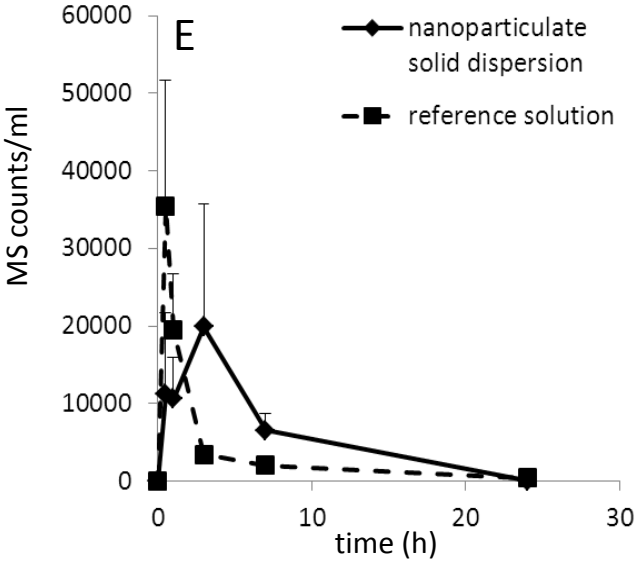
E
nanoparticulate solid dispersion
reference solution
MS counts/ml
time (h)

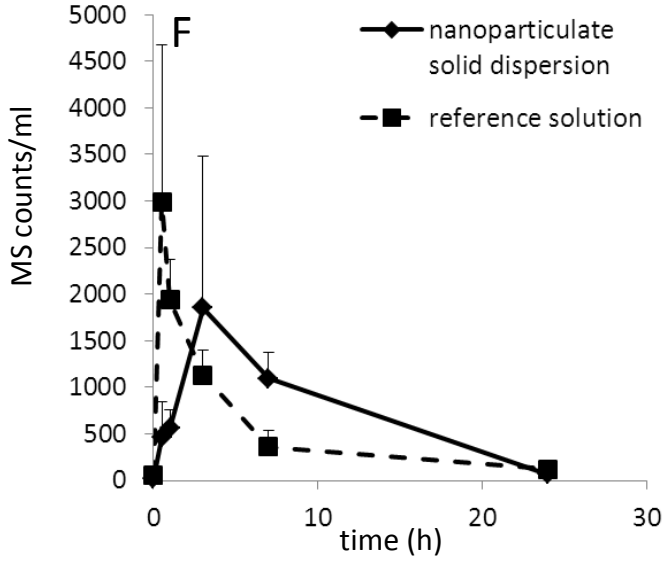
F
nanoparticulate solid dispersion
reference solution
MS counts/ml
time (h)

Figure 8